International Journal of Mathematics Trends and Technology
ISSN: 2231-5373/ https://doi.org/10.14445/22315373/IJMTT-V72I10P108

Volume 72 Issue 10, 93-105, October 2026
© 2026 Seventh Sense Research Group®

Original Article

Fractional Reaction Diffusion Models of Biochemical Signaling Dynamics in Tissue Engineering Systems

Raphael Ebekele George[1], Benjamin Oyediran Oyelami[1,2*], Mary O Durojaye[1,3]

[1]*Department of Mathematics, Yakubu Gowon University, Abuja, Nigeria.*
[2]*Department of Mathematics, National Mathematical Centre, Shelda, Abuja, Nigeria.*

**Corresponding Author : boyelami2000@yahoo.com*

Received: 25 August 2026 Revised: 30 September 2026 Accepted: 18 October 2026 Published: 29 October 2026

Abstract *- This paper presents a time fractional reaction-diffusion model for biochemical signaling dynamics in tissue engineering systems. The model makes use of Jumarie's fractional derivative to capture anomalous molecular transport and long-range memory effects in complex biological environments. The existence and uniqueness of solutions for the models are proved. Analytical closed-form approximate solutions are derived using the Homotopy Analysis Method (HAM) with a Gaussian morphogen initial state. Numerical simulations reveal that when the fractional order parameter* $\alpha < 1$*, the model produces non-local memory effects, delayed sub-diffusive transport, and slower signal propagation. However, as* $\alpha \to 1$*, the model recovers from classical Fickian diffusion behaviour; hence, the solution of the model is consistent with the solution of classical reaction-diffusion models. Parametric sensitivity analysis shows that the baseline diffusion coefficient.* D_0*, nonlinear diffusion strength* β*, and logistic growth parameter* η *collectively influenced the spatial distribution, signal localization, stability, and longevity of morphogen gradients within tissue scaffolds. High diffusion coefficients increase morphogen redistribution through porous biomaterials. Lower diffusion preserves localized signaling in dense media. Elevated logistic growth enhances biochemical signal amplification, while weak growth combined with metabolic degradation suppresses long-term signal persistence. Increased nonlinear diffusion strength intensifies concentration-dependent transport and promotes rapid dispersion in regions of high morphogen density.*

Keywords *- Biochemical signaling, Anomalous diffusion, Fractional reaction diffusion models, Homotopy analysis methods, Tissue engineering.*

1. Introduction

Tissue engineering has appeared as a major interdisciplinary field integrating biology, medicine, materials science, and engineering together to restore, replace, and regenerate damaged tissues and organs [1,2]. Central to successful tissue regeneration is the establishment of effective biochemical signaling environments capable of regulating cellular processes such as proliferation, migration, differentiation, and apoptosis [3,4].

These signaling activities are mediated through the transport of morphogens, cytokines, enzymes, and growth factors within highly heterogeneous biological media [2]. Foundational studies by Langer and Vacanti [1], Place et al. [2], and Discher et al. [3] showed the importance of biochemical signaling and scaffold microstructure in controlling cellular fate and tissue regeneration.

Classical reaction-diffusion equations based on Fickian transport theory have been traditionally used to model biochemical signaling and molecular transport in biological systems [5–7]. These models successfully describe pattern formation and diffusion in homogeneous media [5,6].

Moreover, increasing experimental evidence shows that transport processes in living tissues often deviate from classical diffusion due to extracellular heterogeneity, macromolecular crowding, transient receptor binding, and cellular obstructions [8,9]. Such mechanisms generate anomalous sub-diffusion and nonlocal memory effects that cannot be adequately captured by ordinary differential equations [8–10]. Consequently, conventional reaction–diffusion models often do not accurately describe the spatiotemporal evolution of signaling molecules within complex tissue-engineered environments.

Furthermore, to overcome these limitations, fractional calculus has gained considerable attention as an effective mathematical framework for modeling anomalous transport and hereditary biological processes [8–11]. Fractional-order derivatives naturally incorporate non-local operators and memory kernels, enabling more realistic representations of long-range temporal dependence in biological systems [8,11,12]. Early contributions by Metzler and Klafter [8], Podlubny [9],

This is an open access article under the CC BY-NC-ND license (http://creativecommons.org/licenses/by-nc-nd/4.0/)

Mainardi [10], and Magin [11] demonstrated the effectiveness of fractional operators in describing anomalous diffusion and viscoelastic transport processes. More recently, Diethelm et al. [13] reviewed emerging developments and open problems in fractional calculus, while Magin and Lenzi [14] showed that fractional kinetic formulations significantly improve the description of memory-dependent transport phenomena. Similarly, Dozva et al. [15] surveyed modern computational approaches for solving complex fractional differential equations arising in biological and engineering applications.

The application of fractional reaction–diffusion models to physiological systems has also received growing attention. Tamis and Drapaca [16] developed a space-fractional model for nitric oxide bio transport in brain tissue and showed that fractional operators successfully capture anomalous transport induced by tissue microstructures. Valentim et al. [17] emphasized the importance of non-integer-order calculus in biomedical systems for describing memory-dependent cellular processes, while Ojo and Mahmudov [18] demonstrated the effectiveness of fractional diffusion models in representing nonlocal biological transport dynamics.

Further theoretical developments were presented by Shi et al. [19], who investigated the existence and blow-up behavior of time-fractional reaction-diffusion equations, and by Ghafoor et al. [20], who examined the influence of fractional-order indices on coupled biological and chemical systems. Ahmad et al. [21] extended analytical tools for stability and Turing pattern analysis in fractional reaction-diffusion environments, while Alshehry et al. [22] and Gong et al. [23] highlighted the significant role of fractional diffusion in wave propagation and spatial pattern formation. Collectively, these studies show that fractional reaction-diffusion equations provide a robust framework for modeling complex multiscale biological transport processes that are still difficult to capture using classical integer-order approaches.

Another important feature of biochemical signaling is enzyme-mediated transport and cellular regulation systems. Many signaling pathways involve enzymatic activation, metabolic degradation, and substrate conversion processes that strongly influence morphogen availability and survival. Michaelis–Menten kinetics is still one of the most widely adopted frameworks for describing enzyme–substrate interactions in biological systems [24–26].

It is worth noting that tissue-engineered constructs often show density-dependent cellular regulations that can be effectively represented using logistic growth dynamics [6,7]. These nonlinear mechanisms significantly affect morphogen distribution, signal persistence, and scaffold stability, and therefore must be incorporated into realistic mathematical models of tissue engineering systems.

Motivated by these observations, this study considers a comprehensive time-fractional reaction-diffusion model for biochemical signaling dynamics in tissue engineering environments. The models we will use integrate nonlinear diffusion, Michaelis–Menten enzyme kinetics, metabolic degradation, and logistic cellular regulation within a unified fractional-order derivative framework. The existence and uniqueness of the model solution are proved using the Banach Fixed Point Theorem. To derive analytical approximations, the Homotopy Analysis Method (HAM), originally introduced by Liao [27,28], is employed due to its flexibility in generating convergent series solutions without requiring perturbation assumptions. HAM has been successfully applied to various nonlinear fractional differential equations [29–34], including multidimensional fractional heat equations [32], variable-order systems [33], and hybrid physics-informed computational models [34]. The paper combines fractional-order differential equations and biological concepts for analyzing anomalous morphogen transport and improving biomimetic tissue engineering constructs.

This paper is organized as follows: Section 1 introduction, Section 2 preliminaries, definitions and notations, Section 3 method and Section 4 results and discussion.

2. Preliminaries, Definition and Notations

2.1. Notation

Parameters	Description	Unit
$P(x,t)$	Denotes the continuous spatiotemporal concentration field of signaling morphogens	$mol.mm^{-3}$
$S(x,t)$	Is the spatiotemporal concentration profile of the co-existing reaction substrate available for enzymatic conversion	$mol.mm^{-3}$
K_m	Michaelis constant	$mol.mm^{-3}$
P_c	Specifies the asymptotic environmental carrying capacity threshold	$mol.mm^{-3}$
S_0	Initial substrate concentration	$mol.mm^{-3}$
x	Spatial coordinate	mm
t	Time variable	h
D_0	Baseline intrinsic Fickian diffusion coefficient	$mm^2h^{-\alpha}$
λ	Metabolic degradation rate	$h^{-\alpha}$

η	Intrinsic cellular growth regulation rate	$h^{-\alpha}$
σ	Spatial decay parameter	mm^{-2}
μ	Spatial localization parameter	mm^{-2}
$C_X^2(\Omega)$	Continuous function	
$C_t^{\alpha}(I)$	Holder continuous in t of order α	
I	Time interval	
Ω	Spatial domain	

Based on interrelated bio-transport phenomena, this work considers a fractional reaction-diffusion model for biochemical signaling dynamics in tissue engineering systems which combines nonlinear Fickian transport mechanics, Michaelis-Menten enzyme kinetics, isothermal linear metabolic degradation, and density-dependent logistic self-regulation within a unified time fractional mathematical structure. The governing equation is given as:

$$D_t^{\alpha}P(x,t) = D_0\big(1+\beta P(x,t)\big)\frac{\partial^2 P(x,t)}{\partial x^2} + \frac{V_{max}S(x,t)}{K_m+S(x,t)} - \lambda P(x,t) + \eta P(x,t)\left(1-\frac{P(x,t)}{P_c}\right), 0 \ < \alpha \leq 1 \tag{1}$$

The metric space $X = (\mathbb{C}^2\ (\Omega \times I), \|.\|)$ forms a complete normed linear space and hence constitutes a Banach space.

2.2. Definition of Fractional Operators and Properties

We will make use of the following definitions and fractional calculus operators throughout this work.
The Riemann-Liouville fractional integral of order $\alpha > 0$ for a continuous function $f: [0,\infty) \to \mathbb{R}$ is defined as [9]:

$$I^{\alpha}f(t) = \frac{1}{\Gamma(\alpha)}\int_0^t (t-\tau)^{\alpha-1}f(\tau)d\tau,\ \alpha > 0 \tag{2}$$

The classical Riemann-Liouville fractional derivative of $\alpha\ (n-1) < \alpha \leq n, \in\ \mathbb{N})$ is expressed as:

$$D_t^{\alpha}f(t) = \frac{1}{\Gamma(n-\alpha)}\frac{d^n}{dt^n}\int_0^t (t-\tau)^{n-\alpha-1}f(\tau)d\tau \tag{3}$$

Where $\Gamma(.)$ Represents the standard Euler gamma function.

The Caputo fractional derivative of order $\alpha\ (n-1) < \alpha \leq n, n \in\ \mathbb{N})$ is formulated to incorporate traditional integer-order initial state directly [9]:

$$D_t^{\alpha}f(t) = \frac{1}{\Gamma(n-\alpha)}\frac{d^n}{dt^n}\int_0^t (t-\tau)^{n-\alpha-1}f^{(n)}(\tau)d\tau \tag{4}$$

Guy Jumarie modified Riemann-Liouville fractional derivative and operators of order $\alpha\ (n-1 < \alpha \leq n)$ is defined through a continuous function $f(t)$ as [28]:

$${}_0^J D_t^{\alpha}f(t) = \frac{1}{\Gamma(n-\alpha)}\frac{d^n}{ds^n}\int_0^s (t-\tau)^{n-\alpha-1}(f(\tau)-f(0)d\tau\,, n-1 < \alpha \leq n \tag{5}$$

With the properties

$$D^{\alpha}\left[t^{\beta}\right] = \frac{\Gamma(\beta+1)}{\Gamma(\beta-\alpha+1)}t^{\beta-\alpha}, \beta > o \tag{6}$$

$$I^{\alpha}\left[t^{\beta}\right] = \frac{\Gamma(\beta+1)}{\Gamma(\beta+\alpha+1)}t^{\beta+\alpha}, \beta \geq o \tag{7}$$

$$I^{\alpha}[D_t^{\alpha}P(x,t)] = P(x,t) - P(x,0) \tag{8}$$

3. Methods

3.1. Standardized System Equations

Expanding the spatial derivative of the governing equation by using the standard chain rule, equation (1) becomes:

$$D_t^{\alpha}P(x,t) = D_0\big(1+\beta P(x,t)\big)\frac{\partial^2 P(x,t)}{\partial x^2} + D_0\beta\left(\frac{\partial P(x,t)}{\partial x}\right)^2 + \frac{V_{max}S(x,t)}{K_m+S(x,t)} - \lambda P(x,t) + \ \ \eta P(x,t) - \frac{\eta}{P_c}P^2(x,t) \tag{9}$$

where $P(x,t) \in C_x^2(\Omega) \times C_t^\alpha(I)$ serves as our state variable across space $\Omega \subset \mathbb{R}$ and bounded observation time $I = [0,T]$. For a realistic, localized initialization within the active tissue shell setup, we restrict the system boundaries to a domain through a standardized Gaussian transcendental profile. The initial morphogen state $P(x,0) = f(x)$ and $S(x,t)$ are modeled explicitly as:

$$P(x,0) = f(x) = Ae^{-\mu x^2} \tag{10}$$

$$S(x,t) = S_0 e^{-\sigma x^2} \tag{11}$$

where A stands for the initial peak morphogen focus concentration amplitude, S_0 the spatial baseline substrate presence, and μ, σ are positive spatial attenuation constants.

To solve the nonlinear time fractional partial differential equation, we implement Liao's Homotopy Analysis Method (HAM). We begin by initializing a continuous deformation tracking parameter $q \in [0,1]$ and an explicit convergence control parameter $h \neq 0$.

3.2. Zeroth Order Deformation Equation

Let the initial approximation satisfy. $P_0(x,t) = P(x,0) = f(x)$. We express the nonlinear HAM operator $N[\phi(x,t,q)]$ for any arbitrary tracking function ϕ as:

$$N[\phi(x,t,q)] = D_t^\alpha \phi(x,t,q) - D_0\big(1+\beta\phi(x,t,q)\big)\frac{\partial^2\phi(x,t,q)}{\partial x^2} - \frac{V_{max}S(x,t)}{K_m+S(x,t)} - (\eta-\lambda)\phi(x,t,q) + \frac{\eta}{P_c}\phi^2(x,t,q) \tag{12}$$

We define the auxiliary linear operator as $\mathcal{L}[\phi] = D_t^\alpha \phi$, which satisfies $\mathcal{L}[c] = 0$ for any constant c. Constructing the zeroth-order deformation equation yields:

$$(1-q)\mathcal{L}[\phi(x,t;q) - P_0(x,t)] = qhN[\phi(x,t;q)] \tag{13}$$

Substituting the operator directly into (13) results in the core homotopy relationship:

$$(1-q)D_t^\alpha[\phi(x,t;q) - P_0(x,t)] = qhN[\phi(x,t;q)] \tag{14}$$

Evidently, when $q = 0$, equation (14) simplifies to $\phi(x,t;0) = P_0(x,t)$ and when $q = 1$, it yields $N[\phi(x,t;1)] = 0$, forcing $\phi(x,t;1) = P(x,t)$. Thus, as q sweeps continuously from $0\ to\ 1$, the tracking topology deforms smoothly from the baseline Gaussian initialization to the exact solution.

3.3. The m-th Order Deformation Equation

We expand the function $\phi(x,t;q)$ as a Maclaurin series with respect to the embedding parameter q.

$$\phi(x,t,q) = P_0(x,t) + \sum_{m=1}^{\infty} P_m(x,t)\, q^m \tag{15}$$

Where the m-th derivative part is extracted through:

$$P_m(x,t) = \frac{1}{m!}\frac{\partial^m \phi(x,t;q)}{\partial q^m}\Big|_{q=0} \tag{16}$$

Assuming the auxiliary parameter h is correctly tuned, the series (15) converges exactly at $q = 1$, giving:

$$P(x,t) = P_0(x,t) + \sum_{m=1}^{\infty} P_m(x,t) \tag{17}$$

Differentiating the zeroth-order deformation equation (14) m times with respect to q, dividing by $m!$, and mapping the boundary $q = 0$ yields the m-th order deformation equation:

$$D_t^\alpha P_m(x,t) - X_m D_t^\alpha P_{m-1}(x,t) = hR_m(x,t) \tag{18}$$

Where the scaling factor X_m is defined as:

$$X_m = \begin{cases} 0, & m = 1 \\ 1, & m \geq 2 \end{cases} \tag{19}$$

And the recursive residual part $R_m(x,t)$ is defined as:

$$R_m(x,t) = \frac{1}{(m-1)!}\frac{\partial^{m-1}N[\phi(x,t;q)]}{\partial q^{m-1}}\Big|_{q=0} \tag{20}$$

Applying the Jumarie fractional integration operator I_t^{α} to (18) yields the core recursive engine:

$$P_m(x,t) - X_m P_{m-1}(x,t) = hI_t^{\alpha}[R_m(x,t)] \tag{21}$$

3.4. Derivation of Series Term

We execute the recursive engine sequentially to derive the structural solution components.

3.4.1. First Order Component (P_1)

Setting $m = 1$ in equation (20) and substituting the baseline values yields the first structural residual:

$$R_1(x) = -\left[D_0(1+\beta f)f'' + \frac{V_{max}S(x,t)}{K_m+S(x,t)} + (\eta-\lambda)f - \frac{\eta}{P_c}f^2\right] \tag{22}$$

Because $R_1(x)$ is purely space-dependent, executing the fractional integration step (21) yields:

$$P_1(x,t) = hR_1(x)I_t^{\alpha}[1] = hR_1(x)\frac{t^{\alpha}}{\Gamma(\alpha+1)} \tag{23}$$

Substituting the Gaussian configurations $f(x) = Ae^{-\mu x^2}$ and performing structural algebraic simplification gives:

$$P_1 = \frac{ht^{\alpha}}{\Gamma(\alpha+1)}\left\{Ae^{-\mu x^2}[2\mu D_0 - 4\mu^2 D_0 x^2 - \eta + \lambda] + A^2e^{-2\mu x^2}\left[2\mu\beta D_0 - 4\mu^2\beta D_0 x^2 + \frac{\eta}{p_c}\right] - \frac{V_{max}S_0e^{-\sigma x^2}}{K_m+S_0e^{-\sigma x^2}}\right\} \tag{24}$$

We substitute the standardized compact notation parameter by letting:

$$a = 2\mu D_0 + \lambda - \eta, b = 4\mu^2 D_0, c = 2\mu\beta D_0 + \frac{\eta}{p_c}, d = 4\mu^2\beta D_0 \tag{25}$$

This condenses the structural representation of the first residual to:

$$R_1(x) = Ae^{-\mu x^2}[a - bx^2] + A^2e^{-2\mu x^2}\left[c - 2dx^2 + \frac{\eta}{p_c}\right] - \frac{V_{max}S_0e^{-\sigma x^2}}{K_m+S_0e^{-\sigma x^2}} \tag{26}$$

Where the d term is adjusted to account for the combination of ff'' and $(f')^2$ parts. Thus,

$$P_1(x,t) = \frac{ht^{\alpha}}{\Gamma(\alpha+1)}R_1(x) \tag{27}$$

3.4.2. Second Order Component (P_2)

By we setting $m = 2$ in (20) and executing partial derivative with respect to q yields the second structural residual expression as:

$$R_2(x,t) = D_t^{\alpha}P_1 - D_0(1-\beta f)P_{1,xx} - D_0\beta P_1 f'' - 2D_0\beta f' P_{1,x} + \lambda P_1 - \eta P_1 + \frac{2\eta f}{P_c}P_1 \tag{28}$$

Applying the recursive integration (21) for $m = 2$ yields:

$$P_2(x,t) = P_1(x,t) + hI_t^{\alpha}[R_2(x,t)] \tag{29}$$

Evaluation of the fractional integral term by term and organizing the operators based on their temporal power tracking profiles results in:

$$P_2(x,t) = \frac{(h+h^2)t^{\alpha}}{\Gamma(\alpha+1)}R_1(x) - \frac{h^2D_0t^{2\alpha}}{\Gamma(2\alpha+1)}\left(1+\beta Ae^{-\mu x^2}\right)R_{1,xx} - \frac{h^2D_0\beta t^{2\alpha}}{\Gamma(2\alpha+1)}Ae^{-\mu x^2}(4\mu^2x^2 - 2\mu)R_1(x) - \frac{2h^2D_0\beta t^{2\alpha}}{\Gamma(2\alpha+1)}R_{1,x}(x) - \frac{h^2(\eta-\lambda)t^{2\alpha}}{\Gamma(2\alpha+1)}R_1(x) + \frac{2h^2\eta Ae^{-\mu x^2}t^{2\alpha}}{P_c\Gamma(2\alpha+1)}R_1(x) \tag{30}$$

To compute the final system state, show the analytical structure of the spatial derivative of the first residual. $R_1(x)$.

4. Results

Proposition 1

Let the first residual be defined by (26). Its second spatial derivative $R_{1,xx}$ is given explicitly by the closed form expression for $R_{1,xx}$.

Then :

$$R_{1,xx}(x) = Ae^{-\mu x^2}[-16\mu^4 D_0 x^4 + (48\mu^3 D_0 - 4\mu^2\eta + 4\mu^2\lambda)x^2 + 2\mu\eta - 2\mu\lambda - 12\mu^2 D_0] + A^2 e^{-2\mu x^2}\left[-64\mu^4\beta D_0 x^4 + \left(96\mu^3\beta D_0 + \frac{8\mu^2\eta}{P_c}\right)x^2 - 16\mu^2\beta D_0 - \frac{4\mu\eta}{P_c}\right] + \frac{2\sigma V_{max}K_m S_0 e^{-\sigma x^2}(1-2\sigma x^2)}{\left(K_m + S_0 e^{-\sigma x^2}\right)^2} + \frac{8\sigma^2 x^2 V_{max}K_m S_0^2 e^{-2\sigma x^2}}{\left(K_m + S_0 e^{-\sigma x^2}\right)^3} \quad (31)$$

and

$$P(x,t) \approx P_0(x,t) + P_1(x,t) + P_2(x,t) + \cdots$$

Proof

Given that $f = Ae^{-\mu x^2}$, and $S(x,t) = S_0 e^{-\sigma x^2}$

We begin with the condensed formulation of the first residual tracking equation:

$$R_1(x) = Ae^{-\mu x^2}[2\mu D_0 - 4\mu^2 D_0 x^2 - \eta + \lambda] + A^2 e^{-2\mu x^2}\left[2\mu\beta D_0 - 4\mu^2\beta D_0 x^2 + \frac{\eta}{p_c}\right] - \frac{V_{max}S_0 e^{-\sigma x^2}}{K_m + S_0 e^{-\sigma x^2}} \quad (32)$$

Where $Q(x) = S_0 e^{-\sigma x^2}$. Differentiating equation (32) once with respect to x using the standard product and quotient rules, we get:

$$R_{1,x} = Ae^{-\mu x^2}[8\mu^3 D_0 x^3 + (2\mu\eta - 2\mu\lambda - 12\mu^2 D_0)]x + A^2 e^{-2\mu x^2}\left[16\mu^3\beta D_0 x^3 - \left(16\mu^2\beta D_0 + \frac{4\mu\eta}{p_c}\right)x\right] - \frac{2\sigma K_m S_0 V_{max} x e^{-\sigma x^2}}{\left(K_m + S_0 e^{-\sigma x^2}\right)^2} \quad (33)$$

Differentiating for the second time with respect to x and systematically grouping the variable based on their exponential yields:

$$R_{1,xx}(x) = Ae^{-\mu x^2}[-16\mu^4 D_0 x^4 + (48\mu^3 D_0 - 4\mu^2\eta + 4\mu^2\lambda)x^2 + 2\mu\eta - 2\mu\lambda - 12\mu^2 D_0] + A^2 e^{-2\mu x^2}\left[-64\mu^4\beta D_0 x^4 + \left(96\mu^3\beta D_0 + \frac{8\mu^2\eta}{P_c}\right)x^2 - 16\mu^2\beta D_0 - \frac{4\mu\eta}{P_c}\right] + \frac{2\sigma V_{max}K_m S_0 e^{-\sigma x^2}(1-2\sigma x^2)}{\left(K_m + S_0 e^{-\sigma x^2}\right)^2} + \frac{8\sigma^2 x^2 V_{max}K_m S_0^2 e^{-2\sigma x^2}}{\left(K_m + S_0 e^{-\sigma x^2}\right)^3} \quad (34)$$

Equation(34) shows the value of $R_{1,xx}(x)$ and to complete the proof, we must derive the approximate value for $P(x,t)$.

Summing up, the components derived up to the second order yield total analytical approximation for the morphogen distribution field:

$$P(x,t) \approx P_0(x,t) + P_1(x,t) + P_2(x,t) + \cdots \quad (35)$$

Substituting (24) and (30) directly into (35) provides a fully resolved computation of the considered model:

$$P(x,t) \approx Ae^{-\mu x^2} + \frac{ht^\alpha}{\Gamma(\alpha+1)}\left\{Ae^{-\mu x^2}[2\mu D_0 - 4\mu^2 D_0 x^2 - \eta + \lambda] + A^2 e^{-2\mu x^2}\left[2\mu\beta D_0 - 4\mu^2\beta D_0 x^2 + \frac{\eta}{p_c}\right] - \frac{V_{max}S_0 e^{-\sigma x^2}}{K_m + S_0 e^{-\sigma x^2}}\right\} + \frac{(h+h^2)t^\alpha}{\Gamma(\alpha+1)}R_1(x) - \frac{h^2 D_0 t^{2\alpha}}{\Gamma(2\alpha+1)}\left(1 + \beta A e^{-\mu x^2}\right)R_{1,xx} - \frac{h^2 D_0\beta t^{2\alpha}}{\Gamma(2\alpha+1)}Ae^{-\mu x^2}(4\mu^2 x^2 - 2\mu)R_1(x) - \frac{2h^2 D_0\beta t^{2\alpha}}{\Gamma(2\alpha+1)}R_{1,x}(x) - \frac{h^2(\eta-\lambda)t^{2\alpha}}{\Gamma(2\alpha+1)}R_1(x) + \frac{2h^2\eta A e^{-\mu x^2}t^{2\alpha}}{P_c\Gamma(2\alpha+1)}R_1(x) \quad (36)$$

This ends the proof of Proposition 1.

Lemma 1

Suppose that the following conditions are satisfied:

H1: $P(x,0) = f(x)$ and the substrate field $S(x,t)$ are bound continuous functions such that $\| f \| \leq M$ and $\| S \| \leq S_{max}$.

H2: P_x and P_{xx} are uniformly bounded for any state variable $P \in B_M$, that is, there exist constants $M_1 > 0$ and $M_2 > 0$ such that $\| P_x \| \leq M_1$ and $\| P_{xx} \| \leq M_2$.

H3: Let the nonlinear spatiotemporal differential operator $\mathcal{F}: B_M \to X$ is explicitly defined as:

$$\mathcal{F}[P(x,t)] = D_0\frac{\partial^2 P(x,t)}{\partial x^2} + D_0\beta P(x,t)\frac{\partial^2 P(x,t)}{\partial x^2} + D_0\beta\left(\frac{\partial P(x,t)}{\partial x}\right)^2 + \frac{V_{max}S(x,t)}{K_m + S(x,t)} - \lambda P(x,t) + \eta P(x,t) - \frac{\eta}{P_c}P^2(x,t) \quad (37)$$

We now introduce the mapping of operator T: $B_M \to X$ defined by:

$$T[P(x,t)] = f(x) + \frac{1}{\Gamma(\alpha)}\int_0^t (t-\tau)^{\alpha-1}\mathcal{F}[P(x,t)]d\tau \tag{38}$$

Then $\mathcal{F}[P(x,t)]$ and $T[P(x,t)]$ are bounded operators.

Proof:

Applying the Jumarie fractional integral operator I^{α} to both sides of the structural governing equation and invoking its operational traits yield the nonlinear Volterra integral formulation as follows:

$$P(x,t) = f(x) + \frac{1}{\Gamma(\alpha)}\int_0^t (t-\tau)^{\alpha-1}\mathcal{F}[P(x,t)]d\tau \tag{39}$$

Therefore, a state function $P(x,t)$ is a solution to the fractional reaction diffusion system if and only if it is a fixed point of the operator T satisfying $T[P] = P$.

We proceed with the proof by proving first of all that the operator T maps the closed ball B_M into itself, that is $(T(B_M) \subseteq B_M)$. Taking the absolute value of equation (37) and applying the triangle inequality under the supremum norm to equation (38) yields:

$$\| T[P(x,t)] \| \leq \| f(x) \| + \frac{1}{\Gamma(\alpha)} Sup_{(x,t)\in\Omega\times I} \int_0^t (t-\tau)^{\alpha-1} |\mathcal{F}[P(x,t)]| d\tau \tag{40}$$

To obtain the bound on the integrand, we evaluate the supremum norm of $\mathcal{F}[P(x,t)]$ for any $P(x,t) \in B_M$, as follows:

$$\| \mathcal{F}[P] \| \leq D_0 \| P_{xx} \| + D_0\beta \| P \| \| P_{xx} \| + D_0\beta \| P_x \|^2 + \| \frac{V_{max}S}{K_m+S} \| + \lambda \| P \| + \eta \| P \| + \frac{\eta}{P_c} \| P \|^2 \tag{41}$$

Substituting the values of (M, M_1, M_2, S_{max}) directly into the inequality gives

$$\| \mathcal{F}[P] \| \leq D_0 M_2 + D_0\beta M M_2 + D_0\beta M_1^2 + V_{max} + \lambda M + \eta M + \frac{\eta}{P_c} M^2 = K_0 \tag{42}$$

Where $K_0 > 0$ is a finite positive constant, and substituting this uniform bound back into the operator inequality (42) yields:

$$\| T[P] \| \leq M_0 + \frac{K_0}{\Gamma(\alpha)} \int_0^t (t-\tau)^{\alpha-1} d\tau \tag{43}$$

Evaluating the standard fractional integral analytically:

$$\int_0^t (t-\tau)^{\alpha-1} d\tau = \frac{t^{\alpha}}{\alpha} \tag{44}$$

Thus, over the compact temporal domain bounded by T, we obtain:

$$\| T[P] \| \leq M_0 + \frac{K_0 T^{\alpha}}{\alpha\Gamma(\alpha)} = M_0 + \frac{K_0 T^{\alpha}}{\Gamma(\alpha+1)} \tag{45}$$

To preserve domain invariance, we impose a strict temporal constraint:

$$T \leq \left(\frac{(M-M_0)\Gamma(\alpha+1)}{K_0}\right)^{\frac{1}{\alpha}} \tag{46}$$

Applying constraint (46) to inequality (45) shows that $\|T[P]\| \leq M$. Hence, T maps B_M into B_M. This ends the proof.

Theorem 2

To show a unique fixed point, we must show that the nonlinear operator $\mathcal{F}$ satisfies a Lipschitz condition on B_M.
Let $P(x,t), Q(x,t) \in B_M$ and

$$\mathcal{F}[P] - \mathcal{F}[Q] = D_0(P_{xx} - Q_{xx}) + D_0\beta(PP_{xx} - QQ_{xx}) + D_0\beta((P_x)^2 - (Q_x)^2) - \lambda(P-Q) + \eta(P-Q) - \frac{\eta}{P_c}(P^2 - Q^2) \tag{47}$$

Furthermore, let the following identities be satisfied:

1. For the coupled nonlinear diffusion termQP_{xx}:

$$PP_{xx} - QQ_{xx} = PP_{xx} - QP_{xx} + QP_{xx} - QQ_{xx} = P_{xx}(P-Q) + Q(P_{xx} - Q_{xx}) \tag{48}$$

2. For the gradient squared term:

$$(P_x)^2 - (Q_x)^2 = (P_x - Q_x)(P_x + Q_x) \tag{49}$$

3. For the logistic expansion term:

$$P^2 - Q^2 = (P - Q)(P + Q) \tag{50}$$

Then

$$\mathcal{F}[P] - \mathcal{F}[Q] = D_0(P_{xx} - Q_{xx}) + D_0\beta P_{xx}(P - Q) + D_0\beta Q(P_{xx} - Q_{xx}) + D_0\beta(P_x + Q_x)(P_x - Q_x) - \lambda(P - Q) + \eta(P - Q) - \frac{\eta}{P_c}(P + Q)(P - Q) \tag{51}$$

and $\|f(P) - f(Q)\| \leq L\|P - Q\| \; \forall P, Q \in B_m$.

Proof:

Using the standard properties of derivative bounds in a bounded spatial domain, the differences in spatial derivatives can be controlled by the base state through domain-specific constraints; we have: $\|P_x - Q_x\| \leq C_1\|P - Q\|$ and $\|P_{xx} - Q_{xx}\| \leq C_2\|P - Q\|$. Taking the norm of equation (28) and applying the triangle inequality yields:

$$\|\mathcal{F}[P] - \mathcal{F}[Q]\| \leq \left[D_0C_2 + D_0\beta M_2 + D_0\beta M C_2 + 2D_0\beta M_1 C_1 + |\eta - \lambda| - \frac{2\eta M}{P_c}\right]\|P - Q\| \tag{52}$$

We defined the expression within the brackets as the formal Lipschitz constraint L:

$$L = D_0C_2(1 + \beta M) + D_0\beta(M_2 + 2M_1C_1) + |\eta - \lambda| + \frac{2\eta M}{P_c} \tag{53}$$

Because M, M_1, M_2, C_1, C_2 are all real and bounded, $L < \infty$. Thus, $\mathcal{F}$ satisfies the Lipschitz condition:

$$\|\mathcal{F}[P] - \mathcal{F}[Q]\| \leq L\|P - Q\|, \forall P, Q \in B_M \tag{54}$$

This ends the proof.

Theorem 1(Existence and Uniqueness)

Let $\Omega \; \mathbb{C} \; \mathbb{R}$ denote a bounded spatial domain with boundary Ω, and let $I = [0, T]$

Assume that there exists a constant M, S_{max} such as:

1. $f(x) \in \mathbb{C}^2(\Omega)$, with $\|f\|_{C^2} \leq M$
2. $S(x,t) \in \mathbb{C}(\Omega \times I)$ with $\|S\|_\infty \leq S_{max}$ equipped with the standard supremum norm: $\| P \| = Sup_{x,t\in\Omega\times I}|P(x,t)|$ and $B_m = SP \in X: \|P\|_X \leq M$

The metric space $X = (\mathbb{C}^2 \; (\Omega \times I), \|.\|)$ forms a completely normed linear space and hence constitutes a Banach space.

3. Define the Banach Space $X = \mathbb{C}^2(\Omega \times I)$ equipped with the norm

$\|P\|_X = \|P\|_\infty + \|P_x\|_\infty + \|P_{xx}\|_\infty, \forall P \in \mathbb{C}^2(\Omega \times I)$

Let

$B_M = \{P \in X: \|P\|_X \leq M\}$

And suppose that T is bounded as follows:

$$T \leq \left(\frac{(M - M_0)\Gamma(\alpha+1)}{K_0}\right)^{\frac{1}{\alpha}} \tag{55}$$

and

$$\frac{LT^\alpha}{\Gamma(\alpha+1)} < 1 \tag{56}$$

Then, the nonlinear fractional reaction-diffusion system equation (9) admits a unique solution.

Proof

We now evaluate the contraction mapping criteria for the integral operator T under the supremum norm. Let $P, Q \in B_M$:

$$\|T[P] - T[Q]\| = Sup_{(x,t)\in\Omega\times I}\left|\frac{1}{\Gamma(\alpha)}\int_0^t (t - \tau)^{\alpha-1}\,(F[P(x,\tau)] - \mathcal{F}[Q(x,\tau)])d\tau\right| \tag{57}$$

Applying the uniform Lipschitz bound (56) inside the integral operator yields:

$$\|T[P] - T[Q]\| \leq \frac{L}{\Gamma(\alpha)}\int_0^t (t - \tau)^{\alpha-1}\,\|P - Q\|d\tau \tag{58}$$

Pulling the norm $\|P - Q\|$ outside the temporal integration block and resolving the remaining integral over the maximal domain boundaries $[0, T]$ yields:

$$\|T[P] - T[Q]\| \leq \left[\frac{LT^{\alpha}}{\Gamma(\alpha+1)}\right] \|P - Q\| \tag{59}$$

We defined the contraction constant q as:

$$q = \left[\frac{LT^{\alpha}}{\Gamma(\alpha+1)}\right] \tag{60}$$

According to the Banach Fixed Point Theorem, the operator T defines a strict contraction mapping if

$$q < 1 \Longrightarrow \left[\frac{LT^{\alpha}}{\Gamma(\alpha+1)}\right] < 1 \tag{61}$$

This inequality proves a maximum time horizon T for valid convergence.
Therefore, by Lemma (1-4), it shows that:

1. B_M is complete
2. $T: B_M \to B_M$
3. T is a contraction

Hence, the assumptions of the Banach Fixed Point Theorem are satisfied. Therefore, there exists a unique $P^* \in B_M$ such that
$T[P^*] = P^*$
This implies that $P^*(x,t)$ is a unique solution of the fractional nonlinear reaction-diffusion model on $(\Omega \times I)$. The system is well posed in the sense of existence and uniqueness.
This ends the proof of Theorem 1.

4.1. Numerical Simulation

We will conduct the numerical simulation using Maple 2024 to map the spatiotemporal evolution of the biochemically active signaling morphogen concentration field $P(x,t)$. The baseline parameter configuration used is: $A = 1, \mu = 0.5, D_0 = 0.1, \beta = 0.2, V_{max} = 1 * 10^{-8},\ \sigma = 0.3, K_m = 0.5, \lambda = 0.1, \eta = 0.8, P_c = 10$, and $S_0 = 10$
To study the model response under different environments, we introduce four distinct parametric testing scenarios:

CASE 1: Standard Transport and High Growth Shell $1 \leq t \leq 10$

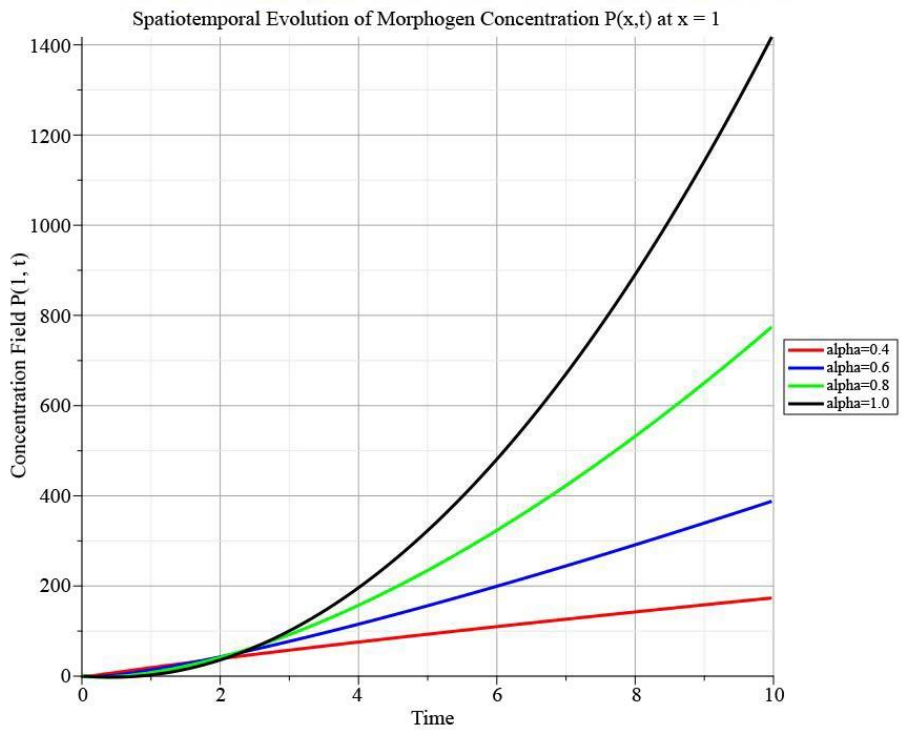

Fig. 1 Morphogen Evolution Concentration at $D_0 = 0.01, and\ \eta = 8$ for different fractional orders. $D_0 = 0.01$, and $\eta = 8$ signal concentration values show monotonic expansion over time across all fractional indices, with $\alpha = 1.0$ showing the highest exponential growth rate; this is the case for ordinary differential equation models.

The primary indicator of anomalous transport behaviour within the system is the fractional memory index α. As illustrated by the numerical trajectories, α from 0.4 up to 1.0 significantly accelerates the temporal evolution of the signaling

field. When $\alpha = 0.4$, the model shows a strong nonlocal memory kernel. The signaling concentration profile adjusts slowly because the immediate transport state is still coupled with historical states. This corresponds physically to a highly heterogeneous shell where subdiffusive delays occur due to macromolecular crowding and binding interactions. Conversely, when $\alpha = 1.0$, the system collapses back into a classical partial differential configuration governed by standard Fickian transport mechanics, displaying rapid redistribution devoid of temporal memory constraints.

CASE 2: Dominant Transport and Weak Production Shell

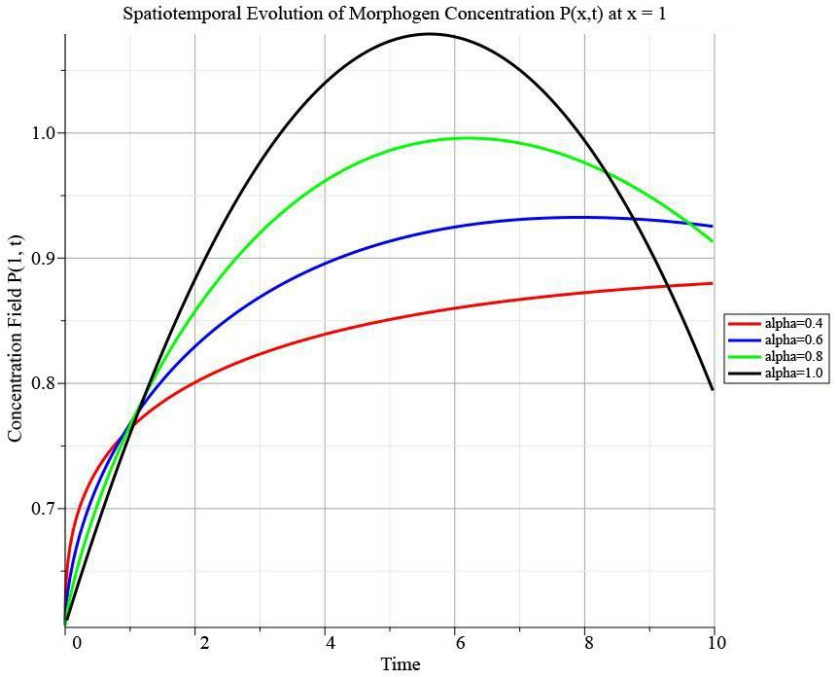

Fig. 2 Morphogen Evolution concentration of $D_0 = 0.1$, and $\eta = 0.008$ trajectories show an initial peak followed by a gradual decay for higher fractional values, while lower indices smooth out the variations. Comparing systems with higher baseline diffusion ($D_0 = 0.1$ against those with restricted transport capability $D_0 = 0.01$ highlights the role of shell structural mechanics. A larger diffusion coefficient speeds up the spatial redistribution of morphogens, smoothing concentration gradients across the medium. In contrast, lower diffusion values isolate signaling molecules near their initial release site. From a tissue engineering standpoint, these profiles map directly onto shell physical traits: high diffusion coefficients are highly porous structural mediums, while low diffusion constants characterize highly dense biomaterial configurations.

CASE 3: Slow Transport and Low Growth Shell

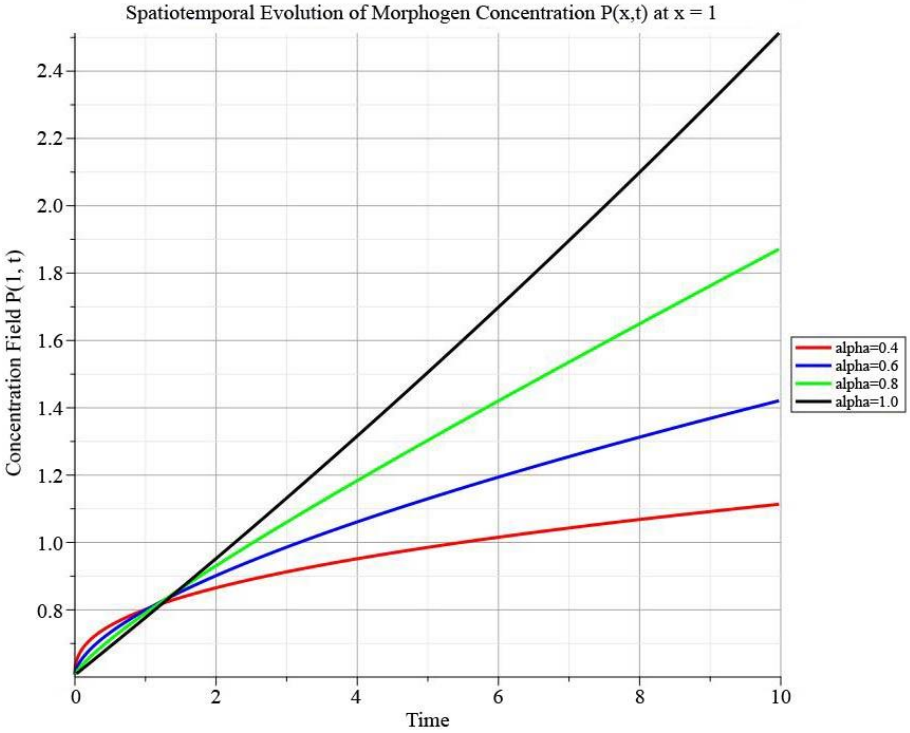

Fig. 3 Morphogen Evolution Concentration at $D_0 = 0.01$ $\eta = 0.008$

Figure 3 shows that the signaling field increases gradually and linearly, displaying severe subdiffusion delays. The contrast between high growth $\eta = 8.0$ and low growth $\eta = 0.008$ media finds logistic regulation as a primary determinant of signal longevity. In high growth setups, rapid biochemical amplification dominates, increasing concentration levels over time. This is a highly active cellular proliferation environment. For low growth configurations, baseline diffusion and linear metabolic degradation dominate, causing a steady decrease in signal intensity over the observation window.

CASE 4: Highly Nonlinear Transport Shell

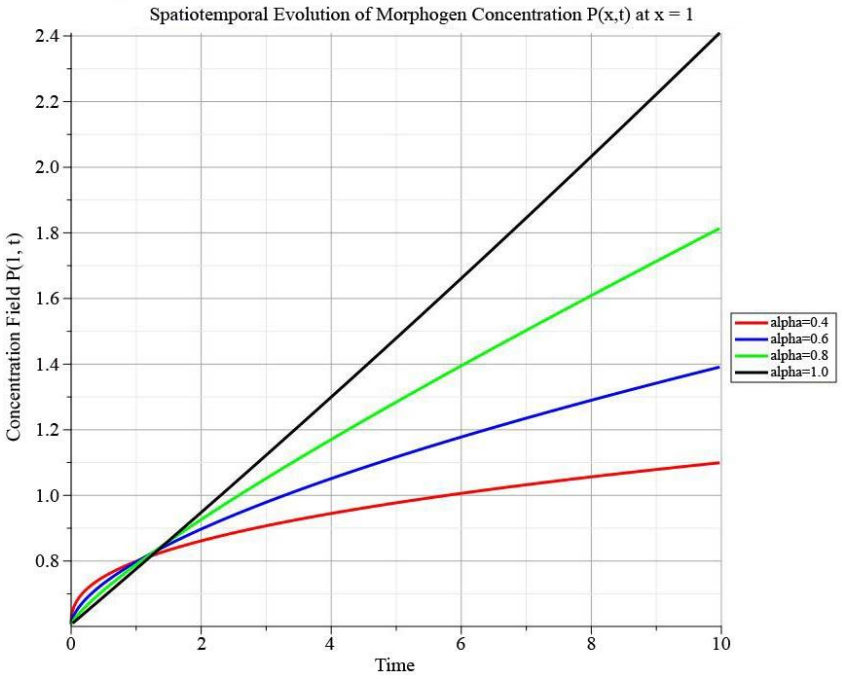

Fig. 4 Morphogen Evolution Concentration at $D_0 = 0.01, \beta = 2$, and $\eta = 0.008$

Figure 4 highlights that elevated concentration-dependent transport mechanics lead to strong signal dispersion in regions of high initial focus. The scaling factor β introduces concentration-dependent transport mechanics. Under weak nonlinearity $\beta = 0.2$, signal propagation follows a standard uniform profile. However, when elevated to $\beta = 2.0$, local transport efficiency scales directly with morphogen concentration. Regions with a high signal density spread rapidly, distorting the concentration profile. This nonlinear coupling allows the model to capture complex, state-dependent transport mechanics common in viscoelastic biological tissues.

5. Conclusion

This work presents a time fractional reaction diffusion model to investigate biochemical signaling dynamics within heterogeneous tissue engineering systems. By integrating Jumarie's modified Riemann-Liouville fractional derivative with nonlinear Fickian transport, Michaelis-Menten kinetics, and logistic self-regulation, Results are obtained that successfully capture nonlocal memory profiles that standard integer-order models cannot resolve. The analytical approximation of the solution is derived through the Homotopy Analysis Method (HAM). Results on the existence and uniqueness of solutions of the fractional-order differential equation are obtained. Parametric sensitivity mappings show that the fractional memory index α directly regulates morphogen propagation velocity and signal longevity. Lower values of α accurately simulate physiological environments where molecular movement is hindered by extracellular matrix complexity, transient receptor binding, and cellular crowding. Furthermore, the analysis reveals that nonlinear diffusion parameters β and logistic amplification rates η jointly govern the stability and spatial localization of signaling profiles. Consequently, this fractional order approach provides a high-reliability predictive background for improving shell pore geometries, designing controlled drug delivery systems, and guiding structural growth factor release in biomimetic regenerative medicine constructs.

Acknowledgements

The first author is a postgraduate student at Yakubu Gowon University, Abuja, Nigeria, and hereby acknowledges support and encouragement received from his mentor and Ph.D. supervisor (second and third authors) and the computational facilities at the University. The second author acknowledges the support received from the University as well as the National Mathematical Centre, Abuja, Nigeria. The third author acknowledges the support received from Yakubu Gowon University, Abuja, Nigeria.

Declaration of Conflict of Interests

The author declared that there was no conflict of interest.

References

[1] Robert Langer, and Joseph P. Vacanti, "Tissue Engineering," *Science*, vol. 260, no. 5110, pp. 920-926, 1993. [CrossRef] [Publisher Link]

[2] Elsie S. Place, Nicholas D. Evans, and Molly M. Stevens, "Complexity in Biomaterials for Tissue Engineering," *Nature Materials*, vol. 8, no. 6, pp. 457-470, 2009. [CrossRef] [Google Scholar] [Publisher Link]

[3] Dennis E. Discher, David J. Mooney, and Peter W. Zandstra, "Growth Factors, Matrices, and Forces Combine and Control Stem Cells," *Science*, vol. 324, no. 5935, pp. 1673-1677, 2009. [CrossRef] [Google Scholar] [Publisher Link]

[4] Adrian Ranga et al., "3D Niche Microarrays for System-Level Analyses of Cell Fate," *Nature Communications*, vol. 5, no. 1, pp. 1-10, 2014. [CrossRef] [Google Scholar] [Publisher Link]

[5] F.R.S. Alan Mathison Turing, "The Chemical Basis of Morphogenesis," *Philosophical Transactions of the Royal Society B*, vol. 237, no. 641, pp. 37-72, 1952. [CrossRef] [Google Scholar] [Publisher Link]

[6] James Dickson Murray, *Mathematical Biology I: An Introduction*, 3rd ed., Springer-Verlag, New York, 2002. [CrossRef] [Google Scholar] [Publisher Link]

[7] John Crank, *The Mathematics of Diffusion*, 2nd ed., Oxford University Press, Oxford, 1975. [Google Scholar] [Publisher Link]

[8] Ralf Metzler, and Joseph Klafter, "The Random Walk's Guide to Anomalous Diffusion: A Fractional Dynamics Approach," *Physics Reports*, vol. 339, no. 1, pp. 1-77, 2000. [CrossRef] [Google Scholar] [Publisher Link]

[9] Igor Podlubny, *Fractional Differential Equations an Introduction to Fractional Derivatives, Fractional Differential Equations, to Methods of Their Solution and Some of Their Applications*, 1st ed., Elsevier, vol. 198, 1998. [Google Scholar] [Publisher Link]

[10] Francesco Mainardi, *Fractional Calculus and Waves in Linear Viscoelasticity*, Imperial College Press, London, 2010. [Google Scholar] [Publisher Link]

[11] Richard L. Magin, *Fractional Calculus in Bioengineering*, 2nd ed., Begell House Publishers, 2006. [Google Scholar] [Publisher Link]

[12] Bruce J. West, Mauro Bologna, and Paolo Grigolini, *Physics of Fractal Operators*, 1st ed., Springer, New York, 2003. [CrossRef] [Google Scholar] [Publisher Link]

[13] Kai Diethelm et al., "Trends, Directions for Further Research, and Some Open Problems of Fractional Calculus," *Nonlinear Dynamics*, vol. 107, no. 4, pp. 3245-3270, 2022. [CrossRef] [Google Scholar] [Publisher Link]

[14] Richard L. Magin, and Ervin K. Lenzi, "Fractional Calculus Modifications to the Kinetic Equations of Statistical Mechanics," *Fractional Calculus and Applied Analysis*, vol. 29, no. 1, pp. 1227-1286, 2026. [CrossRef] [Google Scholar] [Publisher Link]

[15] Robert Dozva, Sicelo P. Goqo, and Shina Daniel Oloniiju, "A Critical Review of Computational Methods for Fractional Differential Equations: Bridging Classical Discretization and Learning-Based Approximations," *Archives of Computational Methods in Engineering*, vol. 33, no. 2, pp. 7571-7594, 2026. [CrossRef] [Google Scholar] [Publisher Link]

[16] Andrew Tamis, and Corina S. Drapaca, "Modeling No Bio Transport in Brain Using a Space Fractional Reaction-Diffusion Equation," *Frontiers in Physiology*, vol. 12, pp. 1-15, 2021. [CrossRef] [Google Scholar] [Publisher Link]

[17] Carlos A. Valentim, José A. Rabi, and Sergio A. David "Fractional Mathematical Oncology: On the Potential of Non-Integer Order Calculus Applied to Interdisciplinary Models," *Biosystems*, vol. 204, 2021. [CrossRef] [Google Scholar] [Publisher Link]

[18] Gbenga O. Ojo, and Nazim I. Mahmudov, "Aboodh Transform Iterative Method for Spatial Diffusion of a Biological Population with Fractional Order," *Mathematics*, vol. 9, no. 2, pp. 1-15, 2021. [CrossRef] [Google Scholar] [Publisher Link]

[19] Linfei Shi et al., "Blow-Up and Global Existence of Solutions for the Time Fractional Reaction-Diffusion Equation," *Mathematics*, vol. 9, no. 24, pp. 1-9, 2021. [CrossRef] [Google Scholar] [Publisher Link]

[20] Abdul Ghafoor et al., "Dynamics of the Time-Fractional Reaction-Diffusion Coupled Equations in Biological and Chemical Processes," *Scientific Reports*, vol. 14, no. 1, pp. 1-25, 2024. [CrossRef] [Google Scholar] [Publisher Link]

[21] Sofwah Ahmad, Szymon Cygan, and Grzegorz Karch, "Tools for Stability Analysis of Fractional Reaction Diffusion Systems," *SIAM Journal on Mathematical Analysis*, vol. 57, no. 2, pp. 891-914, 2025. [Google Scholar]

[22] Azzh Saad Alshehry, Rasool Shah, and Aisha M. Alqahtani, "Analytical Solutions and Dynamic Behavior of Conformable Fractional Reaction-Diffusion Systems," *Scientific Reports*, vol. 16, no. 1, pp. 1-27, 2026. [CrossRef] [Google Scholar] [Publisher Link]

[23] Ying Gong et al., "A Study on the Effects of Riesz Fractional Diffusion on Pattern Formation in a Toxic-Phytoplankton–Zooplankton Model," *Mathematics*, vol. 14, no. 5, pp. 1-20, 2026. [CrossRef] [Google Scholar] [Publisher Link]

[24] Leonor Michaelis, and Maud L. Menten, "The Kinetics of the Inverting Effect," *Biochemical Journal*, vol. 49, pp. 333-369, 1913. [Google Scholar]

[25] Irwin H. Segel, *Enzyme Kinetics: Behavior and Analysis of Rapid Equilibrium and Steady-State Enzyme Systems*, Wiley, 1993. [Publisher Link]

[26] Athel Cornish-Bowden, *Fundamentals of Enzyme Kinetics*, 4th ed., Wiley-Blackwell, 2012. [Google Scholar] [Publisher Link]

[27] Shi-Jun Liao, "*The Proposed Homotopy Analysis Technique for the Solution of Nonlinear Problems*," PhD. Thesis, Shanghai Jiao Tong University, 1992. [Google Scholar]

[28] Shijun Liao, *Homotopy Analysis Method in Nonlinear Differential Equations*, Beijing: Higher Education Press, vol. 153, 2012. [Google Scholar]

[29] Hossein Jafari, and S. Seifi, "Solving a System of Nonlinear Fractional Partial Differential Equations using Homotopy Analysis Method," *Communications in Nonlinear Science and Numerical Simulation*, vol. 14, no. 5, pp. 1962-1969, 2009. [CrossRef] [Google Scholar] [Publisher Link]

[30] Ishak Bin Hashim, O. Abdulaziz, and Shaher M. Momani, "Homotopy Analysis Method for Fractional IVPs," *Communications in Nonlinear Science and Numerical Simulation*, vol. 14, no. 3, pp. 674-684, 2009. [CrossRef] [Google Scholar] [Publisher Link]

[31] Victor Fabian Morales-Delgado et al., "Laplace Homotopy Analysis Method for Solving Linear and Nonlinear Partial Differential Equations of Fractional Order," *Advances in Difference Equations*, vol. 283, pp. 1-14, 2016. [CrossRef] [Google Scholar] [Publisher Link]

[32] Rafał Brociek et al., "An Application of the Homotopy Analysis Method for the Time- or Space-Fractional Heat Equation," *Fractal and Fractional*, vol. 7, no. 3, pp. 1-15, 224. [CrossRef] [Google Scholar] [Publisher Link]

[33] Vivek Mishra, and S. Das, "Solution of Variable Order Fractional Differential Equations Using Homotopy Analysis Method," *Nonlinear Dynamics*, vol. 123, no. 4, pp. 1-11, 2026. [CrossRef] [Google Scholar] [Publisher Link]

[34] Muhammad Azam et al., "A Unified Approach with Physics-Informed Neural Networks (PINNs) and the Homotopy Analysis Method (HAM) for Precise Approximate Solutions to Nonlinear PDEs: A Study of Burgers, Huxley, Fisher and Their Coupled Form," *Symmetry*, vol. 18, no. 3, pp. 1-41, 2026. [CrossRef] [Google Scholar] [Publisher Link]